DESIGN AND PERFORMANCE OF THE BEAM TRANSFER LINES FOR THE HIE-ISOLDE PROJECT

A. Parfenova*, W. Andreazza, J. Bauche, E. D. Cantero, P. Farantatos, M. A. Fraser, B. Goddard, Y. Kadi, A. J. Kolehmainen, D. Lanaia, M. Martino, R. Mompo, E. Siesling, A. G. Sosa, M. Timmins, G. Vandoni, D. Voulot, E. Zografos, CERN, Geneva, Switzerland

Abstract

Beam design and beam optics studies for the HIE-ISOLDE transfer lines [1] have been carried out in MadX [2], and benchmarked against Trace3D results [3, 4]. Magnet field errors and alignment imperfections leading to deviations from design parameters have been treated explicitly, and the sensitivity of the machine lattice to different individual error sources was studied. As a result, the tolerances for the various error-contributions have been specified for the different equipment systems. The design choices for the expected magnet field and power supply quality, alignment tolerances, instrument resolution and physical aperture were validated. The methodology and results of the studies are presented.

INTRODUCTION

The baseline layout contains three identical branch lines as presented in Fig. 1. The large energy range from 0.3 to 10 MeV/u requested for the experiments sets a number of challenging constraints on the beam optics design. The facility is optimized for energies 5.5 and 10 MeV/u. However, some experiments will be carried out at 0.3 MeV/u, where the beam emittance is rather large. Thus the beam transmission at the low energy of 0.3 MeV/u was studied in detail. Errors of different types have been considered and their effects on the machine have been studied and corrected. All simulations were done for a mass-charge ratio A/q=4.5.

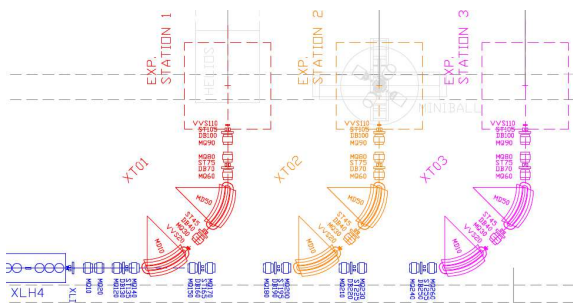

Figure 1: HIE-ISOLDE beam line layout.

TOLERANCES

Magnet field errors and alignment imperfections introduce distortions into the ideal trajectory, detuning and betatron coupling errors, which affect β- and dispersion functions [5]. Different possible error sources of static and dynamic nature were assigned. The impact of each error source was evaluated using MadX simulation; their tolerances are listed in Table 1.

Table 1: Accepted Tolerances for Static Error Sources

Error Source	Value	Distrib.
Dipole field, ΔBdl/Bdl	$1.0 \cdot 10^{-3}$	uniform
roll angle dψ, rad	$1.0 \cdot 10^{-4}$	uniform
longitudinal position dS, m	$1.0 \cdot 10^{-3}$	uniform
Quadrupole field, ΔK/K	$1.0 \cdot 10^{-3}$	uniform
shift dX, dY, m	$2.5 \cdot 10^{-4}$	Gauss(σ)
Initial conditions dX, dY, m	$5.0 \cdot 10^{-4}$	Gauss(σ)
dpx, dpy, mrad	$5.0 \cdot 10^{-4}$	Gauss(σ)
Monitor shift dX, dY, m	$2.5 \cdot 10^{-4}$	Gauss(σ)
resolution X, Y, m	$2.0 \cdot 10^{-4}$	uniform

Dipole and quadrupole power ripple are the main sources of dynamic errors: accepted tolerances for ΔI/I are of the order 10^{-4} at 5.9 MeV/u (and higher energies) and of the order 10^{-3} at 0.3 MeV/u (up to $7 \cdot 10^{-3}$ for some quadrupoles). At 0.3 MeV/u dynamic errors introduce a dilution to the X-beam spot at the target with a sigma of 0.3 mm (Fig. 2).

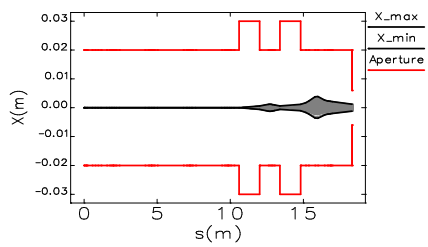

Figure 2: X-trajectory distortion due to dipole power ripple at the low energy (0.3 MeV/u).

CORRECTION OF STATIC ERRORS

Piecewise Trajectory Correction (10 MeV/u)

Trajectory correction is essential to minimize beam loss. Trajectory distortion from residual misalignment and field errors (static errors) was corrected by a piecewise algorithm. The piecewise correction is a combination of segment-by-segment corrections done over a short range consecutively alternating steerers one by one and correcting the trajectory at the next monitor downstream of the steerer.

* angelina.parfenova@cern.ch

ISBN 978-3-95450-122-9

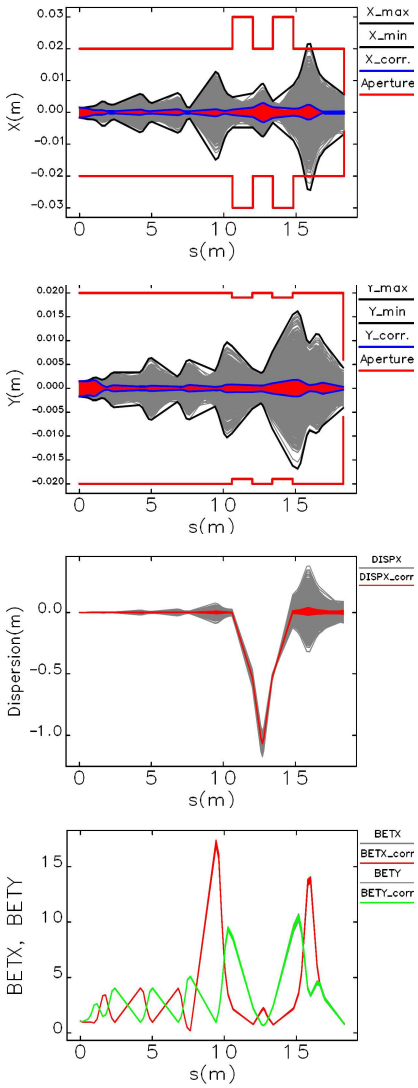

Figure 3: X-/Y- trajectories, dispersion and β-functions before/after piecewise trajectory correction of all static errors (1000 seeds). Data plots were done in SDDS-toolkit [6].

The simulation for each seed shown in Fig. 3 includes following steps

- including static errors,
- generating optics and trajectory,
- correcting trajectory,
- recalculating optics and corrected trajectory.

Steerer strengths used in the correction are less than $\pm$ 2 mrad, which are within the foreseen steering power.

Orthogonal Steering (10 MeV/u)

After the trajectory correction of the beam centroid there still exists a finite divergence in (x, x', y, y') at the target, which can be corrected to zero (x = y = x' = y' = 0) by a unique setting of two correction angles of the two last steerers before the target (orthogonal steering). The complementary correction angles found in 1000 seeds simulation for the two steerers are within $\pm$ 0.4 mrad.

The maximum possible correction angles of the two steerers without intersecting with the beam aperture and exceeding their maximum design strengths put limits on the acceptable error in position and tilt of the target axis. The maximum correction angles are specified by the beam envelope of two sigma starting to hit the aperture (Fig. 4), where the one sigma beam size is defined by

$$\sigma_x = \sqrt{\epsilon_x \cdot \beta_x + (\sigma_{\Delta p/p} \cdot D_x)^2},\ \sigma_y = \sqrt{\epsilon_y \cdot \beta_y}. \quad (1)$$

Available phase-space area (x,x') and (y, y') is shown in Fig. 5.

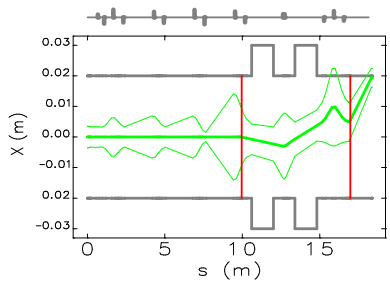

Figure 4: Two sigma beam envelope hitting the aperture. Red vertical lines indicate steerer positions.

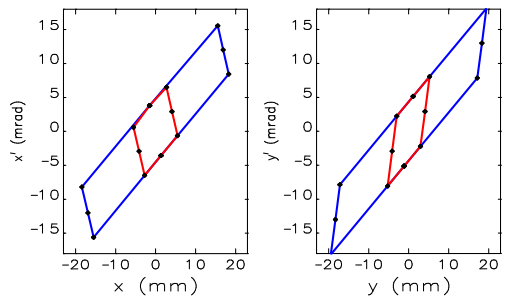

Figure 5: The limits at the target are defined by the physical aperture (blue line) and by the maximum strength of steerers at 10 MeV/u (red line).

BEAM TRANSMISSION AT 0.3 MEV/U

Tracking of the particle distribution [4] was done with ptc_track module of MadX [2]. Beam sizes calculated from Twiss parameters [4] by using beam parameters for 0.3 MeV/u ϵ_x = 2.91 $\cdot$ 10^{-6} m, ϵ_y = 2.91 $\cdot$ 10^{-6} m, $\sigma_{\Delta p/p}$ = 2.68 $\cdot$ 10^{-3} (solid line) and from tracking (dots) are in agreement for both X-/Y- planes (Fig. 6) that shows that particle dynamics is very well represented by the linear optics.

A tracking simulation for many error seeds was carried out. Introduced static errors were corrected. Dynamic errors at 0.3 MeV/u (Fig. 2) were introduced on top of the

ISBN 978-3-95450-122-9

correction. The beam loss along the beam line averaged over 100 error seeds is presented in Fig. 7. A reasonably low average beam loss of 0.3% was found.

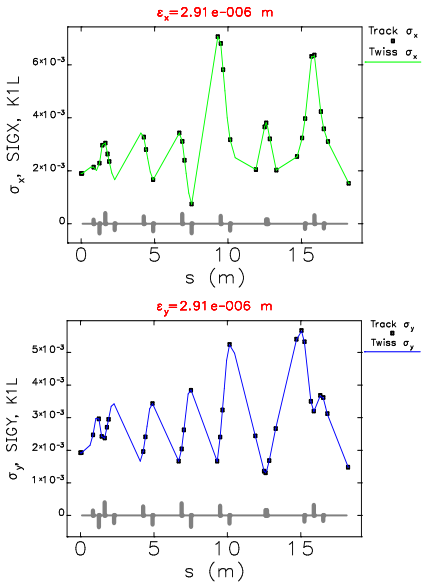

Figure 6: One sigma beam sizes $\sigma_{x/y}$ of Eq. (1) calculated from Twiss (solid line) and from tracking (dots) for both X-/Y- planes, respectively (ideal trajectory).

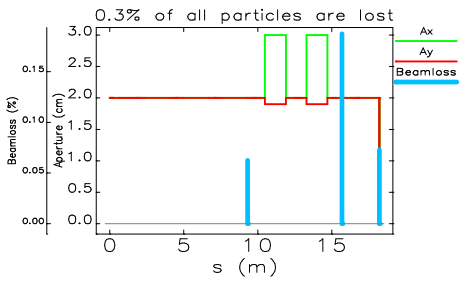

Figure 7: Beam loss distribution along the beam line averaged over 100 error seeds.

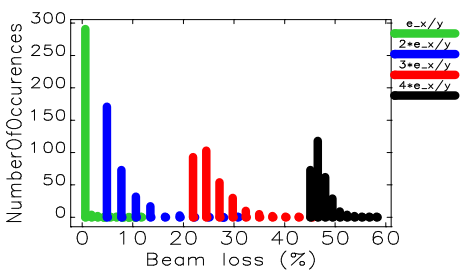

Figure 8: Beam transmission histogram as a function of the beam emittance for 300 error seeds.

To study the dependence of beam loss on beam emittance, larger beams were produced from the original particle distribution at 0.3 MeV/u by multiplying the coordinates (x, x', y, y') by $\sqrt{2}$, $\sqrt{3}$ and $\sqrt{4}$, sequentially. Transmission histograms as a function of the beam emittance for 300 error seeds are plotted in Fig. 8. For the double and triple beam emittances the average beam loss found is 6.9% and 25.3%, respectively.

BEAM SIZES AT THE TARGET

Estimated average X-/Y- beam spots at the target defined as 4σ in Eq. (1) are about 2.7 mm at 10 MeV/u (Fig. 9); 3 mm at 5.9 MeV/u and 6 mm at 0.3 MeV/u with the dilution of 0.3 mm from the power ripple of dipole and quadrupole magnets. The estimated beam spot sizes meet the requested design values for experiments at higher energies as the machine was optimised for the beams in the range 5.5 to 10 MeV/u.

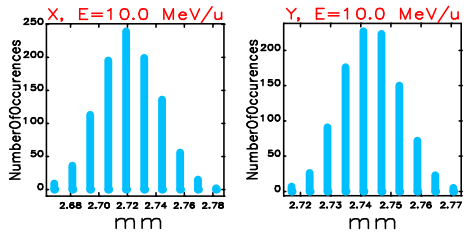

Figure 9: Estimated X-/Y- beam spots at the target obtained after the piecewise trajectory correction of all static errors.

ACKNOWLEDGMENT

The authors thank W. Herr, A. Petrenko, G. Franchetti, L. Dienau, F. Schmidt and W. Bartmann for scientific discussions, programming tips and benchmarking of MadX tools. We acknowledge funding from the Belgian Big Science program of the FWO (Research Foundation Flanders) and the Research Council K.U. Leuven. We would like to acknowledge as well the receipt of fellowships from the CATHI Marie Curie Initial Training Network: EU-FP7-PEOPLE-2010-ITN Project number 264330.

REFERENCES

[1] D. Voulot et al., "HIE-ISOLDE SC Linac: Operational Aspects and comissioning preparation", IPAC'2012, New Orleans, Louisiana, USA, THPPP050, p. 3853 (2012).

[2] F. C. Iselin, *The MAD Program, Methodical Accelerator Design*, CERN, Geneva, Switzerland, 2000, `http://mad.web.cern.ch/mad/`.

[3] K. R. Crandall et al., *TRACE 3-D Documentation*, Los Alamos National Laboratory, New Mexico, USA, 1997, `http://laacg1.lanl.gov`.

[4] M. Fraser, *Beam Dynamics Studies of the ISOLDE Post-accelerator for the High Intensity and Energy Upgrade*, PhD Thesis, Manchester, U.K., 2012, 167.

[5] S. Y. Lee, *Accelerator Physics*, World Scientific, Singapore, 2004, 85.

[6] M. Borland et al., "The Self-Describing Data Sets File Protocol and Program Toolkit", Proc. ICALEPCS 1995, Chicago, Illinois, USA, pp. 653 (1996), `http://www.aps.anl.gov/asd/oag/software.shtml`.